Transition-State Spectroscopy via Negative Ion Photodetachment

DANIEL M. NEUMARK

Department of Chemistry, University of California, Berkeley, California 94720, and Chemical Sciences Division,
Lawrence Berkeley Laboratory, Berkeley, California 94720

Received July 13, 1992

Introduction

One of the most ambitious goals in the field of reaction dynamics is to be able to construct the complete potential energy surface for a chemical reaction. Given such a surface, one can, in principle, calculate all attributes of the reaction, down to the most detailed state-to-state cross section. Thus, in recent years, an array of experimental and theoretical methods has been developed with the goal of extracting chemically accurate potential energy surfaces for reactions. This is a daunting problem; at present, the $H + H_2$ reaction is the only system for which such a surface is available. However, while the construction of a full potential energy surface is certainly desirable, it seems more reasonable to concentrate on the regions of the surface that play the largest role in determining the dynamics of a chemical reaction. A fundamental concept in physical chemistry is the idea of the transition state of a reaction, a dividing surface between reactants and products. The transition state often acts as a "bottleneck" in a chemical reaction, with the consequence

Daniel Neumark was born on March 27, 1955, in Chicago, IL. He was an undergraduate at Harvard University and graduated in 1977 with a B.A. in chemistry and physics and an M.A. in chemistry. While at Harvard, he received his first exposure to the world of molecular beams and reaction dynamics through his undergraduate research experience with Prof. Dudley Herschbach. He then spent a year at Cambridge University working with Professor A. D. Buckingham. He received his Ph.D. from the University of California, Berkeley, in 1984 under the supervision of Prof. Yuan Lee; his thesis work concerned the dynamics of the F + H₂ reaction. From 1984 to 1986, he was a postdoctoral fellow at the University of Colorado, Boulder, where he worked for Prof. Carl Lineberger on autodetachment spectroscopy of negative ions. He returned to Berkeley in 1986 as a faculty member and is currently Associate Professor of Chemistry. His research program is centered on using negative ions as precursors for studies of the spectroscopy and dynamics of unstable and/or highly reactive species.

that many of the measurable properties of a reaction, ranging from differential cross sections to rate constants, are largely determined by the nature of the potential energy surface in the vicinity of the transition state. Thus, experiments which directly probe this transition-state region can provide detailed insight into the most important part of the reaction potential energy surface, enabling us to learn about the microscopic, interatomic forces that control chemical reactivity.

These considerations have made the development of workable "transition-state spectroscopy" schemes a high priority in reaction dynamics. The first experiments of this type were performed by Polanyi[1] and Brooks.[2] These were scattering experiments based on the idea that one could directly probe the colliding reactants near the transition state via emission or absorption. The experiments are quite challenging. The transition state is an unstable molecular configuration, which is, in general, very short-lived, on the order of 10^{-13}–10^{-15} s. Thus, the steady-state concentration of transition region species in a scattering experiment is extremely small. In addition, reactive collisions typically occur over a wide range of reactant orientations and orbital angular momentums, and the spectroscopy of the resulting transition region species, even when measurable, is difficult to interpret. Because of these considerations, relatively few studies of transition region species formed in bimolecular collisions have been reported in recent years.[3,4]

A more popular approach to transition-state spec-

(1) Arrowsmith, P.; Bartoszek, F. E.; Bly, S. H. P.; Carrington, T., Jr.; Charters, P. E.; Polanyi, J. C. J. Chem. Phys. 1980, 73, 5895–7.
(2) Hering, P.; Brooks, P. R.; Curl, R. F.; Judson, R. S.; Lowe, R. S. Phys. Rev. Lett. 1980, 44, 687–90.
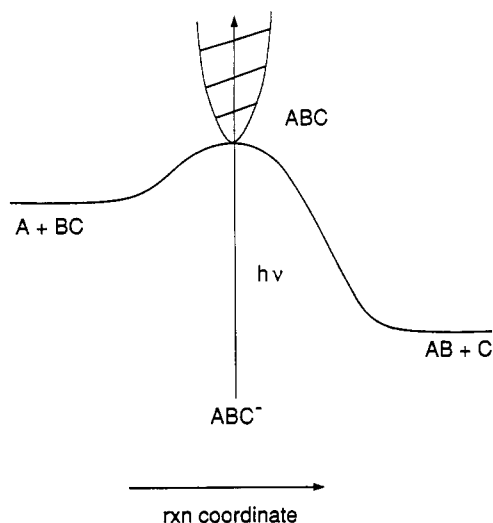
Figure 1. One-dimensional idealization of transition-state spectroscopy experiment.

troscopy over the last several years has been to form transition region species not by a collision but by photoexcitation of a stable species. This largely eliminates the averaging over reactant initial conditions that occurs in the scattering-based studies. Notable examples include the experiments of Imre et al.[5] in which the emission from dissociating fragments is monitored, the work of Soep and co-workers[6] in which electronic excitation of a van der Waals complex initiates an excited-state chemical reaction, and the elegant time-resolved experiments performed by the Zewail group.[7] Both types of transition-state spectroscopy experiments have been extensively reviewed.[8-10] This article focuses on transition-state spectroscopy experiments done in our research group, which are also of the second type. In these experiments, the transition state of a neutral, bimolecular reaction is accessed by photodetachment of a stable negative ion.

Before discussing our experiments in any detail, it is worth considering the goals of a transition-state spectroscopy experiment. Figure 1 shows the potential energy along an idealized reaction coordinate for a direct, bimolecular reaction A + BC → AB + C where there is a small barrier between reactants and products. The classical transition state for this reaction is at the top of this barrier. The barrier is, in reality, a saddle point on a multidimensional potential energy surface. At the transition state, the potential energy surface is

bound along coordinates perpendicular to the reaction coordinate and can therefore support vibrational levels where the nuclear motions are constrained to these bound coordinates. Both the barrier height and the frequencies of these transition-state vibrational levels play important roles in the dynamics of the reaction. Both appear in the transition-state theory rate constant, for example:[11]

$$k(T) = \frac{kT}{h} \frac{Q_I^*}{Q_I Q_T} \exp(-E_0/kT) \qquad (1)$$

Here, E_0 is the classical barrier height, and Q_I^* is the partition function for the internal (rotational and vibrational) degrees of freedom at the transition state, excluding translation along the reaction coordinate. (Q_I and Q_T are the internal and translational partition functions, respectively, for the reactants.) Equation 1 is only an approximation, in that it assumes that the rate constant depends *only* on the properties of the potential energy surface at the transition state. It does, however, emphasize the importance of learning about both the barrier height *and* the vibrational motion of the complex formed when two reactant molecules collide.

Now, suppose the anion ABC⁻ is stable and has a geometry close to that of the ABC transition state. Then, as shown in Figure 1, photodetachment of ABC⁻ results in an ABC neutral complex which lies in the transition-state region of the A + BC potential energy surface. The actual experiment we perform, in most cases, is photoelectron spectroscopy. In these experiments,[12] the anion is photodetached with a fixed-frequency laser and the kinetic energy distribution of the resulting photoelectrons is measured with about 10-meV (80 cm⁻¹) resolution.

In most anion photoelectron spectroscopy experiments, the neutral formed by photodetachment is stable, and the spectrum consists of a series of sharp peaks corresponding to transitions to vibrational levels associated with various electronic states of the neutral. For example, Figure 2 shows the photoelectron spectrum of NO₂⁻.[13] The spectrum consists of transitions to various bending (ν_2) and symmetric stretch (ν_1) vibrational levels of the ground electronic state of NO₂. The electron kinetic energy (eKE) at which each transition occurs is determined by

$$eKE = h\nu - EA(NO_2) - E_{int}(NO_2) + E_{int}(NO_2^-) \qquad (2)$$

where $h\nu$ is the photon energy (3.49 eV in this spectrum), EA(NO₂) is the electron affinity of NO₂, and $E_{int}(NO_2)$ and $E_{int}(NO_2^-)$ are the internal (vibrational and rotational) energies of NO₂ and NO₂⁻, respectively. Note that peaks at lower kinetic energy correspond to transitions to more highly excited NO₂ levels. The intensity of each peak is determined by square of the overlap (i.e., the Franck–Condon factor) between the anion and neutral vibrational wave functions.

The situation in Figure 1 is quite different. Photodetachment will access vibrational levels of the transition-state complex, ABC, but these levels are, in most

(3) Barnes, M. D.; Brooks, P. R.; Curl, R. F.; Harland, P. W. *J. Chem. Phys.* **1991**, *94*, 5245-7. Barnes, M. D.; Brooks, P. R.; Curl, R. F.; Harland, P. W.; Johnson, B. R. *J. Chem. Phys.* **1992**, *96*, 3559-68.

(4) Kleiber, P. D.; Lyrra, A. M.; Sando, K. M.; Zafiropoulos, Z.; Stwalley, W. C. *J. Chem. Phys.* **1986**, *85*, 5493-504. Bililign, S.; Kleiber, P. D.; Kearney, S. R.; Sando, K. M. *J. Chem. Phys.* **1992**, *96*, 218-29.

(5) Imre, D. G.; Kinsey, J. L.; Field, R. W.; Katayama, D. H. *J. Phys. Chem.* **1982**, *86*, 2564-6. Imre, D. G.; Kinsey, J. L.; Sinha, A.; Krenos, J. *J. Phys. Chem.* **1984**, *88*, 3956-64.

(6) Breckenridge, W. H.; Jouvet, C.; Soep, B. *J. Chem. Phys.* **1986**, *84*, 1443-50. Soep, B.; Whitham, C. J.; Keller, A.; Visticot, J. P. *Faraday Discuss. Chem. Soc.* **1991**, *91*, 191-205.

(7) Gruebele, M.; Roberts, G.; Zewail, A. H. *Philos. Trans. R. Soc. London, A* **1990**, *332*, 223-43. Zewail, A. H. *Faraday Discuss. Chem. Soc.* **1991**, *91*, 207-37.

(8) Brooks, P. R. *Chem. Rev.* **1988**, *88*, 407-28.

(9) Zewail, A. H. *Science* **1988**, *242*, 1645-53. Gruebele, M.; Zewail, A. H. *Physics Today* **1990**, *43*, 24-33. Zewail, A. H. *Faraday Discuss. Chem. Soc.* **1991**, *91*, 207-37.

(10) Metz, R. B.; Bradforth, S. E.; Neumark, D. M. *Adv. Chem. Phys.* **1992**, *81*, 1-61. Neumark, D. M. *Annu. Rev. Phys. Chem.* **1992**, *43*, 153-76.

(11) Eyring, H. *J. Chem. Phys.* **1935**, *3*, 107-15.

(12) Metz, R. B.; Weaver, A.; Bradforth, S. E.; Kitsopoulos, T. N.; Neumark, D. M. *J. Phys. Chem.* **1990**, *94*, 1377-88.

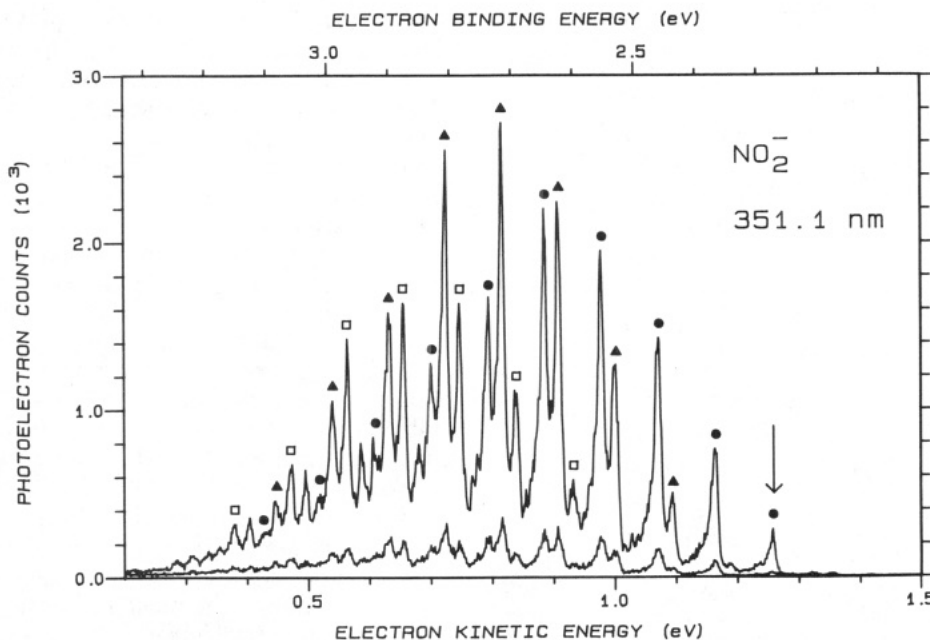(13) Ervin, K. M.; Ho, J.; Lineberger, W. C. *J. Phys. Chem.* **1988**, *92*, 5405-12.

Figure 2. Photoelectron spectrum of NO_2^-. The origin (0_0^0 transition) is indicated with an arrow. Progressions in the ν_1 symmetric stretch and ν_2 bending mode are labeled as follows: $1_0^0 2_0^n$ progression (●), $1_0^1 2_0^n$ progression (▲), $1_0^2 2_0^n$ (□). The subscripts and superscripts are the vibrational quantum numbers in NO_2^- and NO_2, respectively. Reprinted with permission from ref 15. Copyright 1988 American Chemical Society.

cases, *unbound* along the reaction coordinate, so the complex typically dissociates quite rapidly. However, since the complex is bound along coordinates perpendicular to the reaction coordinate, it will undergo vibrational motion as it dissociates. So long as this vibrational motion perpendicular to the reaction coordinate occurs on the same time scale as, or faster than, dissociation, we will observe a structured photoelectron spectrum in which the peaks correspond to vibrational levels of the ABC complex at or near the transition state. This is brought out more quantitatively in the time-dependent wavepacket analysis described later in this Account (eqs 4–6). Roughly speaking, the longer the complex holds together, the narrower the peaks in the photoelectron spectrum will be. Thus, the peak positions and widths are a measure of the spectroscopy *and* dissociation dynamics of the transition-state complex. It is worth emphasizing that although Figure 1 allows one to visualize why vibrational structure can be observed in our experiments, more realistic pictures of reaction potential energy surface are needed in order to interpret our results in any detail.

We conclude the Introduction by noting that one can improve on the resolution obtained in photoelectron spectroscopy by using a different technique, threshold photodetachment spectroscopy.[14] Here, the anions are photodetached with a tunable laser, and only those electrons produced with nearly zero kinetic energy are collected as a function of laser frequency. This, in principle, yields the same information as photoelectron spectroscopy, namely, the energies of vibrational and electronic levels of the neutral formed by photodetachment, but at considerably higher resolution (0.3–0.4 meV). A comparison of results from the two methods is presented in the following section.
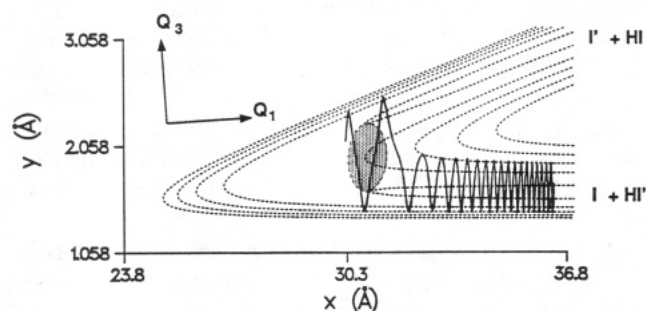

Figure 3. Collinear potential energy surface for I + HI reaction from ref 15 plotted in mass-weighted coordinates: $x = (\mu_{I,HI}/\mu_{HI})^{1/2}(R_I - R_{cm}(HI'))$, $y = R_H - R_{I'}$. The axes corresponding to the symmetric (Q_1) and antisymmetric (Q_3) normal coordinates are also shown. The Franck–Condon region is shaded, and a sample classical trajectory that originates near the Franck–Condon region is shown.

The I + HI Reaction

As the first example of this type of experiment, we consider the symmetric hydrogen exchange reaction I + HI → HI + I. A collinear model potential energy surface[15] for this reaction is shown in Figure 3. The surface is plotted in mass-weighted coordinates (see figure caption); also shown are the directions of Q_1 and Q_3, the symmetric and antisymmetric stretch normal coordinates, respectively, for the IHI complex. We probe the transition-state region for this reaction by photodetaching the IHI⁻ anion. This is a linear, strongly hydrogen-bonded anion ($D_0 = 0.74$ eV[16]) which can be pictured, to zero order, as a proton holding two I⁻ anions together. Photodetachment of IHI⁻ is a vertical process, meaning that the nuclear geometry immediately after photodetachment is the same as in the anion. Hence, photodetachment "lands" us onto a region of the neutral potential energy surface centered at the anion equi-

(14) Kitsopoulos, T. N.; Waller, I. M.; Loeser, J. G.; Neumark, D. M. *Chem. Phys. Lett.* **1989**, *159*, 300–6.

(15) Manz, J.; Römelt, J. *Chem. Phys. Lett.* **1981**, *81*, 179–84.
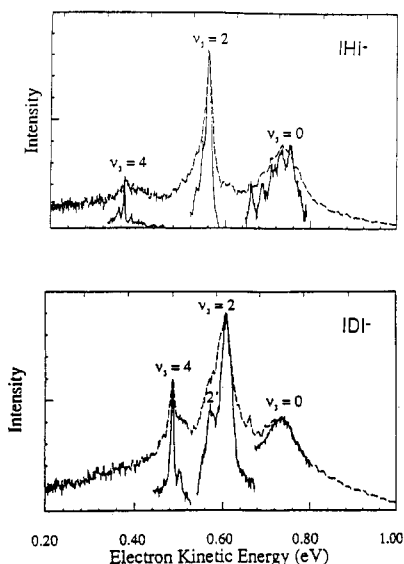(16) Caldwell, G.; Kebarle, P. *Can. J. Chem.* **1985**, *63*, 1399–406.

Figure 4. Photoelectron spectra of IHI⁻ and IDI⁻ taken a photon energy $h\nu$ = 4.66 eV (dashed lines). Also shown is a higher resolution threshold photodetachment spectrum of IHI⁻ (solid lines).

librium geometry (estimated R_{II} = 3.88 Å[17]), the extent of this region being determined by the zero-point amplitude of the vibrations in the anion. This region, called the "Franck–Condon region", is shaded in Figure 3. It is the region probed in the most detail when IHI⁻ is photodetached. A very important consideration in these experiments is that the Franck–Condon region should include or lie close to the classical transition state; this is the case for IHI⁻ and all the other examples discussed later.

In order to understand what occurs on the I + HI surface subsequent to IHI⁻ photodetachment, it is useful to consider the classical trajectories that will be followed by IHI complexes formed in (or near) the Franck–Condon region. An example of such a trajectory[18] is shown in Figure 3. As the I atoms move apart along the Q_1 coordinate, the complex undergoes several large amplitude oscillations along the Q_3 coordinate before becoming confined to the I + HI' valley. This large amplitude motion corresponds to the antisymmetric stretch mode of the IHI complex, in which the H atom is vibrating between two essentially stationary I atoms. Thus, relating Figure 3 to Figure 1, bound motion of the IHI complex occurs along the Q_3 antisymmetric stretch coordinate, while the dissociation of the complex occurs along the Q_1 symmetric stretch coordinate. Hence, the IHI⁻ photoelectron spectrum should exhibit vibrational structure associated with the antisymmetric stretch of the IHI complex.

This expectation is borne out by the experimental IHI⁻ and IDI⁻ photoelectron spectra in Figure 4.[17] Each spectrum shows three well-resolved peaks. The peak spacing is noticeably less in the IDI⁻ spectrum; this strong isotope shift is expected for a progression in the antisymmetric stretch of the neutral complex. The three peaks in each spectrum are assigned to transitions to the ν_3 = 0, 2, and 4 antisymmetric stretch levels of

the IHI (IDI) complex as shown in Figure 4.[19] (Recall that features at high electron kinetic energy correspond to low energy levels of the neutral.) Another significant feature is that the peak spacings in the photoelectron spectra are substantially less than the HI (or DI) vibrational frequencies. The ν_3 = 0 and 2 peaks in the IHI⁻ spectrum are separated by 1000 cm⁻¹, while the HI fundamental is around 2300 cm⁻¹. This "red shift" occurs because the potential along the Q_3 coordinate is considerably shallower in the transition-state region than in the asymptotic (reactant or product) regions of the surface; the hydrogen atom is interacting strongly with both I atoms in the transition-state region, as illustrated in Figure 3. Hence, we are indeed observing vibrational structure associated with the region of the potential energy surface where chemical bonds are being broken and formed.

These qualitative considerations have been borne out in a variety of quantum mechanical simulations of the IHI⁻ photoelectron spectrum on model I + HI potential energy surfaces. In most of these simulations, the photoelectron spectrum $\sigma(E)$ is generated by calculating the Franck–Condon factors between the initial anion state, $\Psi_{\nu'}{}^{(-)}$ (generally assumed to be the ground vibrational state of the anion), and the neutral scattering wave function, $\Psi^{(0)}(E)$, supported by the I + HI potential energy surface:

$$\sigma(E) \propto |\langle \Psi^{(0)}(E)|\Psi_{\nu'}{}^{(-)}\rangle|^2 \qquad (3)$$

The most difficult part of eq 3 is the determination of the scattering wave function $\Psi^{(0)}(E)$, which, in an exact simulation of the spectrum, must be obtained for the full three-dimensional I + HI potential energy surface. Exact simulations have been performed by Schatz,[20] while more approximate simulations, some of which are restricted to collinear IHI geometries, have been performed by Bowman[21] and by our group.[17] All the simulations show extended progressions in the IHI antisymmetric stretch, in agreement with experiment.

As discussed in the Introduction, one can learn about the dissociation dynamics of the IHI complex from the peak widths. However, this requires that the peaks widths in the photoelectron spectrum are due to the lifetime of the complex rather than originating from unresolved, overlapping transitions. The resolution of the photoelectron spectrum in Figure 4 is about 10 meV, and to check if there is underlying structure, we have also obtained the higher resolution (~0.4 meV) threshold photodetachment spectrum of IHI⁻ and IDI⁻.[22,23] These results are also shown in Figure 4.

The higher resolution spectra show the ν_3 = 2 and 4 peaks in IHI⁻ split into progressions with a characteristic spacing of about 100 cm⁻¹. This result is consistent with the aforementioned simulations and several other studies[24] that predict that the I + HI potential energy surface supports vibrational levels that not only are

(17) Weaver, A.; Metz, R. B.; Bradforth, S. E.; Neumark, D. M. *J. Phys. Chem.* **1988**, *92*, 5558–60.

(18) Skodje, R. T.; Davis, M. J. *J. Chem. Phys.* **1988**, *88*, 2429–56.

(19) The ν_3 = 2′ peak in the IDI⁻ spectrum is associated with the opening of the I + DI(ν=1) channel and is discussed in detail in ref 23.

(20) Schatz, G. C. *J. Chem. Phys.* **1989**, *90*, 4847–54; *J. Phys. Chem.* **1990**, *94*, 6157–64.

(21) Bowman, J. M.; Gazdy, B. *J. Phys. Chem.* **1989**, *93*, 5129–35. Gazdy, B.; Bowman, J. M. *J. Chem. Phys.* **1989**, *91*, 5615–24.

(22) Waller, I. M.; Kitsopoulos, T. N.; Neumark, D. M. *J. Phys. Chem.* **1990**, *94*, 2240–2.

(23) Metz, R. B.; Neumark, D. M. *J. Chem. Phys.* **1992**, *97*, 962–77.

(24) Pollak, E. *J. Chem. Phys.* **1983**, *78*, 1228–36. Manz, J.; Meyer, R.; Schor, H. H. R. *J. Chem. Phys.* **1984**, *80*, 1562–8.

Transition-State Spectroscopy

Acc. Chem. Res., Vol. 26, No. 2, 1993 **37**

bound along directions perpendicular to the IHI dissociation coordinate (the symmetric stretch), like the levels depicted in Figure 1, but also are quasi-bound *along* this coordinate. These quasi-bound states undergo one or more vibrations along the symmetric stretch prior to dissociation and, for IHI, are expected to have a vibrational frequency of about 100 cm^{-1}, in agreement with our observations. The significance of the states derives from their role in the dynamics of the I + HI reaction; they lead to sharp features in the (calculated) I + HI reaction cross section as a function of energy. The existence of these features, called "reactive resonances", has been predicted for some time,[25,26] and our results represent their first definitive experimental observation. The resonances associated with the ν_3 = 4 level of IHI are only 30 cm^{-1} wide, indicating lifetimes of at least 180 fs for the complex.

Figure 4 also shows that the ν_3 = 0 feature in the IHI$^-$ photoelectron spectrum also splits into several features at higher resolution. The characteristic spacing of these peaks increases in the direction of higher IHI excitation from 160 to 200 cm^{-1}, and therefore the states associated with them are quite different from the quasi-bound states associated with the ν_3 = 2 and 4 peaks. The ν_3 = 0 peaks have been assigned to internal rotor levels of the IHI complex.[20,22,23] Basically, when the IHI(ν_3 = 0) level is formed, internal rotation of one of the HI moieties occurs on the same time scale as dissociation of the complex, giving rise to the peaks in the higher resolution spectrum. Overall, the threshold photodetachment spectra yield a substantially richer picture of the transition-state spectroscopy of the I + HI reaction.

The Br + HI Reaction

We next consider applications of our transition-state spectroscopy method to more chemically interesting reactions. As an example, we can study the reaction Br + HI → I + HBr by photoelectron spectroscopy of BrHI$^-$. The photoelectron spectra of BrHI$^-$ and BrDI$^-$ are shown in Figure 5.[28] Each spectrum shows two vibrational progressions, the origins of which are separated by about 1 eV. Within each progression, the peak spacing is noticeably less in the BrDI$^-$ spectrum than in the BrHI$^-$ spectrum, indicating, as was the case for IHI$^-$, that the dominant vibrational structure is due to H atom motion in the neutral complex. However, the BrHI$^-$ peak spacings are only 200 cm^{-1} less, on the average, than the HBr fundamental, a much smaller "red shift" relative to diatomic products than was seen in the IHI$^-$ spectrum.

Although the spectra in Figure 5 can be analyzed within the time-independent framework of eq 3, it is instructive to use a somewhat different approach: the time-dependent wavepacket formalism developed by Heller.[27] In this type of simulation, one determines the time evolution of an initial wavepacket $\phi(t = 0)$ created by photodetachment; at any later time t, the wavepacket $\phi(t)$ is given by

(25) Truhlar, D. G.; Kuppermann, A. *J. Chem. Phys.* **1970**, *52*, 3841–3. Levine, R. D.; Wu, S.-F. *Chem. Phys. Lett.* **1971**, *11*, 557–61.
(26) Schatz, G. C. *Annu. Rev. Phys. Chem.* **1988**, *39*, 317–40 and references therein.
(27) Heller E. J. *J. Chem. Phys.* **1978**, *68*, 3891–6; *Acc. Chem. Res.* **1981**, *14*, 368–75.
(28) Bradforth, S. E.; Weaver, A.; Arnold, D. W.; Metz, R. B.; Neumark, D. M. *J. Chem. Phys.* **1990**, 7205–22.
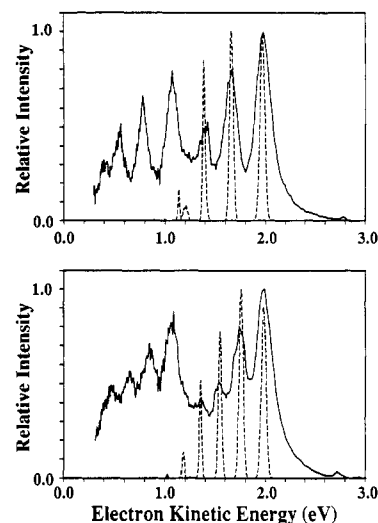

Figure 5. Photoelectron spectra of BrHI$^-$ (top) and BrDI$^-$ (bottom) taken at $h\nu$ = 5.82 eV (solid lines). Simulations from time-dependent wavepacket analysis are also shown (dashed lines).

$$|\phi(t)\rangle = \exp[-i\hat{H}t/\hbar]|\phi(0)\rangle \qquad (4)$$

where $\hat{H}$ is the Hamiltonian on the I + HI surface. The determination of $\phi(t)$ is the most difficult part of the problem; in our simulations,[28] we use the propagation scheme developed by Kosloff[29] to find $\phi(t)$. One then determines the time-autocorrelation function

$$C(t) = \langle\phi(0)|\phi(t)\rangle \qquad (5)$$

which is the overlap of the wavepacket at time t with the initial wavepacket $\phi(0)$. The photoelectron spectrum is given by the Fourier transform of $C(t)$:

$$\sigma(E) \propto \int_{-\infty}^{\infty} \exp(iEt/\hbar)\, C(t)\, dt \qquad (6)$$

In comparison to the time-independent analysis discussed above (eq 3), the time-dependent approach is more computationally demanding, but it provides a stronger link with the simple classical picture in Figure 3. In the Franck–Condon approximation, $\phi(0)$ is the initial anion wave function projected onto the neutral potential energy surface. Loosely speaking, the time evolution of $\phi(0)$, determined from eq 4, resembles the classical trajectory in Figure 3; $\phi(t)$ oscillates along the Q_3 coordinate as it bifurcates into reactants and products. This leads to oscillations in time in $C(t)$ and, consequently, peaks in the photoelectron spectrum $\sigma(E)$.

Let us now apply this type of analysis to the simulation of the BrHI$^-$ and BrDI$^-$ spectra, using a model Br + HI potential energy surface[30] and restricting ourselves to collinear geometries. Figure 6 shows the initial wavepacket $\phi(0)$ superimposed on this surface. (The determination of the anion wave function is discussed in ref 28.) This wavepacket is localized mainly on the product (I + HBr) side of the saddle point, because the anion geometry is asymmetric, with $R_{H-Br} < R_{H-I}$. The wavepacket $\phi(t)$ at several later times, obtained using eq 4, is also shown. At early times ($t \le$ 80 fs), we see substantial motion of the wavepacket along the y axis, corresponding to H–Br vibrational

(29) Kosloff, D.; Kosloff, R. *J. Comput. Chem.* **1983**, *52*, 35–53.
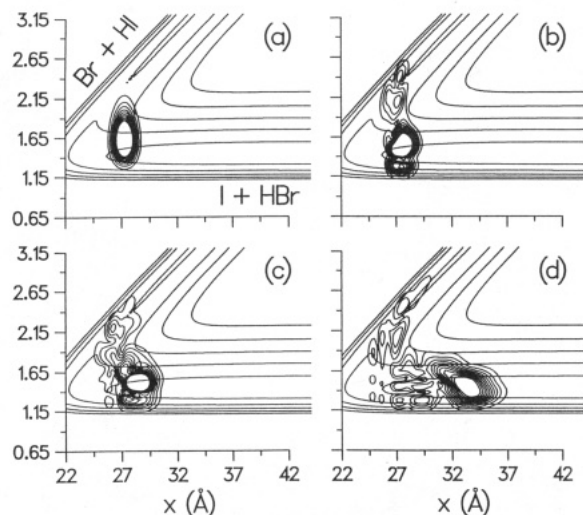(30) Broida, M.; Persky, A. *Chem. Phys.* **1989**, *133*, 405–13.

Figure 6. Wavepacket dynamics on the Br + HI collinear surface: (a) initial wave function $\phi(0)$, which is the BrHI$^-$ ground state projected onto the Br + HI surface; (b–d) evolution of the wave function at later times t = 40.3, 100.7, and 201.3 fs, calculated using eq 4.
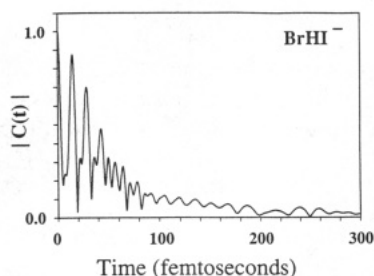

Figure 7. Plot of modulus of $|C(t)|$ vs time (see eq 5), showing time evolution of wavepacket $\phi(0)$ in Figure 6.

motion. At later times, the bulk of the wavepacket moves out in the product valley to form I + HBr. The wavepacket dynamics are concisely displayed in Figure 7, a plot of $|C(t)|$ (see eq 5) vs time. This shows rapid oscillations at early time due to the H atom vibrational motion, and it decays at later time as the BrHI complex dissociates. The simulated photoelectron spectrum, shown in Figure 5, is obtained by taking the Fourier transform of $C(t)$ according to eq 6.

The simulations line up reasonably well with the experimental progression at higher energy. The simulated peaks are too narrow, but a more recent analysis by our group[23] shows that this is at least partly due to the restriction to collinear geometries. The progression at lower electron kinetic energy, which corresponds to the formation of neutral BrHI with *higher* internal excitation, does not appear in the simulated spectrum. It is due to transitions to a different electronic state: an electronically excited Br + HI surface that correlates to I*($^2P_{1/2}$) + HBr products. The spin-orbit excited I*($^2P_{1/2}$) state lies 0.94 eV above the I($^2P_{3/2}$) ground state, and this is very close to the separation between the two vibrational progressions in the BrHI$^-$ spectrum. The wavepacket simulations explain why the peak spacing in the photoelectron spectrum is similar to but slightly less than the vibrational frequency in diatomic HBr. The initial wavepacket is formed on the product side of the classical transition state, so the early time dynamics of the BrHI complex correspond approximately to vibrational motion of a perturbed HBr molecule.
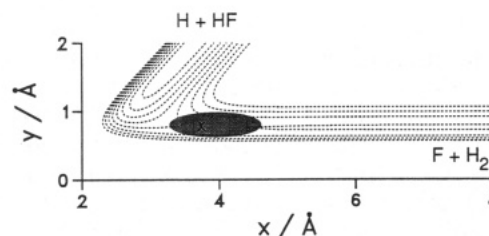

Figure 8. Collinear section of the T5a potential energy for the F + H$_2$ reaction with the Franck–Condon region shaded.

The BrHI$^-$ photoelectron spectrum is an example of what happens when photodetachment primarily accesses the product (i.e, exothermic) side of a reactive potential energy surface. Both the vibrational and the electronic structure in the spectrum can be associated with properties of the I + HBr products. A similar situation arises in photodetachment of all of the asymmetric anions XHY$^-$ (X ≠ Y).[10,28] On the other hand, we have also studied a series of hydrogen abstraction reactions by fluorine, in which the precursor anion has much better geometric overlap with the saddle point and/or the reactant side of the neutral surface. These include the F + OH, F + CH$_3$OH, and F + H$_2$ reactions, studied via photoelectron spectroscopy of OHF$^-$, CH$_3$OHF$^-$, and FH$_2^-$.[31,32] Due to space limitations, only the last of these will be discussed in this Account.

The F + H$_2$ Reaction

Next to the H + H$_2$ reaction, the F + H$_2$ reaction is perhaps the most fundamental in the field of reaction dynamics. In many ways, progress in the field mirrors the experimental and theoretical advances developed in studies of this reaction.[33] In contrast to the reactions discussed above, a considerable amount of effort has been devoted to developing an accurate potential energy surface for the F + H$_2$ reaction.[34] It is therefore a tempting target for our transition-state spectroscopy experiments. Ab initio calculations[35] show that the precursor anion, FH$_2^-$, is essentially F$^-$ weakly bound to H$_2$, so that photodetachment should access the reactant side of the F + H$_2$ potential energy surface. From the ab initio geometries and vibrational frequencies for the anion, we find the Franck–Condon region on the F + H$_2$ surface to be as shown in Figure 8, centered on the reactant side of the saddle point.

The photoelectron spectrum of FH$_2^-$ is shown in Figure 9.[32] The spectrum shows several partially resolved features which, on the basis of their behavior with respect to isotopic substitution, are clearly vibrational features associated with the FH$_2$ complex. Exact, three-dimensional simulations (with total angular momentum J = 0) of the FH$_2^-$ spectrum have been performed by Zhang et al.[36] using the T5a potential

(31) Bradforth, S. E.; Arnold, D. W.; Metz, R. B.; Weaver, A.; Neumark, D. M. *J. Phys. Chem.* **1991**, *95*, 8066–78.

(32) Weaver, A.; Neumark, D. M. *Faraday Discuss. Chem. Soc.* **1991**, *91*, 5–16.

(33) Levine, R. D.; Bernstein, R. B. *Molecular Reaction Dynamics and Chemical Reactivity*, Oxford: New York, 1987; pp 397–411.

(34) Schaeffer, H. F. *J. Phys. Chem.* **1985**, *89*, 5336–43.

(35) Nichols, J. A.; Kendall, R. A.; Cole, S. J.; Simons, J. *J. Phys. Chem.* **1991**, *95*, 1074–6.

(36) Zhang, J. Z. H.; Miller, W. H. *J. Chem. Phys.* **1990**, *92*, 1811–8. Zhang, J. Z. H.; Miller, W. H.; Weaver, A.; Neumark, D. M. *Chem. Phys. Lett.* **1991**, *182*, 283–9.
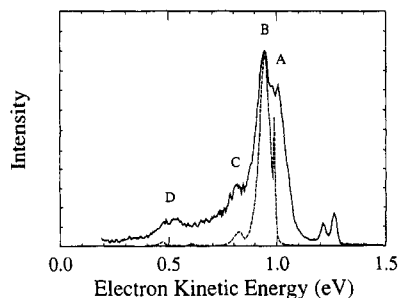
Figure 9. FH_2^- photoelectron spectrum (solid line) taken at $h\nu$ = 4.66 eV with simulation (dashed line) from ref 36.

energy surface[37] for $F + H_2$. The simulation, calculated by means of eq 3, is also shown in Figure 9. There is clearly qualitative agreement between the experimental and simulated spectra. Each of the four peaks in the simulation lines up with an experimental peak. This indicates that the T5a surface is reasonably accurate in the Franck–Condon region. The interpretation of the peaks in the FH_2^- spectrum is not as straightforward as in the BrHI⁻ and IHI⁻ spectra; for example, the FH_2^- spectrum does not show clear progressions in a single vibrational mode of the neutral complex. On the basis of a comparison with reactive scattering calculations on the T5a surface,[36,38] we assigned peaks A and D to a resonance, that is, an FH_2 state which is quasi-bound along the reaction coordinate, while peaks B and C were assigned to transitions to unbound vibrational FH_2 levels of the type shown in Figure 1.

There are several areas of disagreement between the experimental and simulated spectra. The simulated features are too narrow, and there appear to be additional peaks in the experimental spectrum. These discrepancies likely are due in part to inadequacies in the T5a surface. Reactive scattering calculations have recently been performed[39] on a newer $F + H_2$ surface,

the 5SEC surface,[40] which has a smaller barrier than the T5a surface (1.67 vs 2.97 kcal/mol) and a small van der Waals well in the entrance valley. These calculations suggest that the small peak between peaks A and B, rather than peak A itself, is due to the resonance and that, overall, simulations of the FH_2^- spectrum on the 5SEC surface (which have yet to be performed) may be in better agreement with experiment. In any case, the photoelectron spectroscopy studies clearly provide a new experimental "handle" that will prove invaluable in gaining a detailed understanding of the $F + H_2$ reaction dynamics and potential energy surface.

Summary

In this Account, we have briefly described three examples in which negative ion photodetachment is used to probe the transition-state region of a bimolecular reaction. The examples illustrate that photoelectron spectroscopy and threshold photodetachment spectroscopy can yield vibrational structure and dissociation dynamics associated with the transition state. The three examples also show the importance of anion geometry, as this determines which region of the neutral potential energy surface is accessible via photodetachment. This last point is, in fact, one of the most important limitations of these experiments. One way to mitigate this problem is to perform photoelectron spectroscopy studies on vibrationally excited anions. Photodetachment of these anions will probe different vibrational levels and geometries of the neutral transition state. Such studies are planned for the near future.

(37) Steckler, R.; Truhlar, D. G.; Garrett, B. C. *J. Chem. Phys.* **1985**, *82*, 5499–505.

(38) Yu, C.; Kouri, D. J.; Zhao, M.; Truhlar, D. G.; Schwenke, D. W. *Chem. Phys. Lett.* **1989**, *157*, 491–5. Bacic, Z.; Kress, J. D.; Parker, G. A.; Pack, R. T. *J. Chem. Phys.* **1990**, *92*, 2344–61.

(39) Kress, J. D.; Hayes, E. F. *J. Chem. Phys.* **1992**, *97*, 4881–9.

(40) Lynch, G. C.; Steckler, R.; Schwenke, D. W.; Truhlar, D. G.; Varandas, A. J. C.; Garrett, B. C. *J. Chem. Phys.* **1991**, *94*, 7136–49.